Published in final edited form as:
Biochemistry. 2010 March 9; 49(9): 2068–2074. doi:10.1021/bi902089w.

Small Molecular, Macromolecular and Cellular Chloramines React with Thiocyanate to Give the Human Defense Factor Hypothiocyanite†

Bheki A. Xulu and **Michael T. Ashby***
Department of Chemistry and Biochemistry, University of Oklahoma, Norman, OK 73019

Abstract

Thiocyanate reacts non-catalytically with myeloperoxidase-derived HOCl to produce hypothiocyanite ($OSCN^-$), thereby potentially limiting the propensity of HOCl to inflict host tissue damage that can lead to inflammatory diseases. However, the efficiency with which SCN^- captures HOCl *in vivo* depends on the concentration of SCN^- relative to other chemical targets. In blood plasma, where the concentration of SCN^- is relatively low, proteins may be the principal initial targets of HOCl, and chloramines are a significant product. Chloramines eventually decompose to irreversibly damage proteins. In the present study, we demonstrate that SCN^- reacts efficiently with chloramines in small molecules, in proteins, and in *Escherichia coli* cells to give $OSCN^-$ and the parent amine. Remarkably, $OSCN^-$ reacts faster than SCN^- with chloramines. These reactions of SCN^- and $OSCN^-$ with chloramines may repair some of the damage that is inflicted on protein amines by HOCl. Our observations are further evidence for the importance of secondary reactions during the redox cascades that are associated with oxidative stress by hypohalous acids.

Organismic oxidative stress involves complex redox cascades that inflict wide-spread damage to cells and tissue constituents (1). Hypohalites (including OCl^-, OBr^-, and $OSCN^-$), in particular, are implicated in human health and disease (2–6). Hypohalites are produced by the oxidation of halides (or a pseudo-halide, as in the case of SCN^-) with hydrogen peroxide in reactions that are catalyzed by the human peroxidases; including lactoperoxidase (LPO), salivary peroxidase, myeloperoxidase, and eosinophil peroxidase(7); primarily for the purpose of combating host infection:

$$X^- + H_2O_2 \xrightarrow{\text{peroxidase}} OX^- + H_2O \ (X=Cl, Br, SCN) \quad (1)$$

The relative oxidation potentials of the halides are: $Cl^- > Br^- > SCN^-$. Thus, SCN^- may serve as a scavenging agent *in vivo* for the more powerful oxidants hypochlorous acid (X = Cl) (8) and hypobromous acid (X = Br) (9), in reactions that also yield $OSCN^-$ (10):

$$HOX + SCN^- \rightarrow OSCN^- + X^- + H^+ \quad (2)$$

†This work was funded by the National Science Foundation (CHE-0911328) and the National Institutes of Health (1 R21 DE016889-01A2).

*To whom correspondence should be addressed. Tel: 405-325-2924. Fax: 405-325-6111. MAshby@ou.edu.

Supporting Information Available: Mathematica code (used to fit the data of Figure 3), Figure S1 (analogous to Figure 2, albeit for different reaction conditions) and Figures S2–S9 (representative time-resolved spectral data used to vet the "kinetic signature" of $OSCN^-$ and quantify the [$OSCN^-$] in various samples). This material is available free of charge via the Internet at http://pubs.acs.org.

These and related non-catalytic reactions, such as the reaction of HOX with the antioxidant glutathione (11–13), are believed to restrict the lifetimes of HOX, and thereby limit their propensities to inflict host tissue damage that can lead to inflammatory diseases (2–6).

The second-order rate constants for the reactions of HOX with SCN^- are very large (10^7 and 10^9 $M^{-1}s^{-1}$ for X = Cl and Br, respectively) (8,9), but the efficiency with which SCN^- captures HOX (X = Cl and Br) *in vivo* depends upon its concentration relative to other chemical targets. The [SCN^-] in various human physiologic fluids depends upon the source of the fluid and any smoking habits of the individual. We have suggested that eq 2 dominates in the oral cavity (where [SCN^-] is mM) (14), but a recent study of conditions similar to those of human plasma (where [SCN^-] is μM) suggests that HOCl would preferentially react with proteins (15). The protein chloramines, that are a significant initial product of HOCl-mediated protein oxidation, eventually undergo further reactions, including hydrolysis to carbonyls, one-electron reductions to N-centered radicals, and chlorine transfer reactions (including some that are directed towards protein residues by the protein tertiary structure) (16). In the present study, we demonstrate that chloramines also react with SCN^- to give $OSCN^-$ (R = small molecule, protein, or cellular component; Figure 1):

$$RNHCl + SCN^- + H_3O^+ \xrightarrow{k_1} RNH_3^+ + OSCN^- + Cl^- \quad (3)$$

Thus, SCN^- is capable of repairing some of the damage to proteins that is caused by HOCl, but at a cost of producing potentially injurious $OSCN^-$ (17,18).

Experimental Section

Materials

All chemicals were A.C.S certified grade or better, and were used as received from Sigma-Aldrich. Water was doubly distilled in glass. Unless otherwise stated, all solutions were prepared using 0.1 M phosphate buffer at pH 7.4 (I = 1.0). The buffer was prepared using $NaH_2PO_4 \cdot H_2O$ and Na_2HPO_4. The ionic strength was adjusted with NaCl. Stock solutions of NaOCl were prepared by sparging Cl_2 into a 0.3 M solution of NaOH. The sparging was stopped when the [OCl^-] achieved approximately 100 mM (pH 12), as determined spectrophotometrically ($\varepsilon(OCl^-)_{292nm}$ = 350 $M^{-1}cm^{-1}$).

Instrumental Measurements and Data Analysis

UV-vis spectra were collected using an Ocean Optics UBC2000 CCD spectrometer equipped with a 1 meter WPI fiber optic cell and an ATS D 1000 CE UV light source. pH measurements were made with an Orion Ion Analyzer EA920 using a Ag/AgCl combination pH electrode. Kinetic measurements were made using a Bio-Logic SFM-400/Q mixer and a MOS-450 spectrophotometer equipped with a Xe arc lamp and a PMT detector. Single-mixing mode was used for all the stopped-flow experiments. The pseudo-second-order rate constants were obtained by nonlinear least-squares fits of the data with KaleidaGraph 3.6 (Synergy Software) or by Euler's method using Mathematica 7.0 code (for Figure 3), available in the Supporting Information. All stopped-flow kinetic traces represent the average of at least nine mixing cycles.

Preparation of TauCl

A 2.5 mM stock solution of TauCl solution, free of dichloramine ($TauCl_2$) and excess taurine (Tau), was prepared by adding 5.0 mM OCl^- in 0.10 M NaOH dropwise to 5.0 mM Tau in 0.10 M NaOH while vortexing (19). The formation of TauCl was confirmed by observation of the characteristic absorbance spectrum (ε_{252nm} = 429 $M^{-1}cm^{-1}$). Solutions of TauCl in 0.10

M phosphate buffer were prepared from the stock solution by adjusting the pH to 7.4 using a 10 mM solution of HCl.

Reaction of TauCl with SCN^- and Quantification of $OSCN^-$

Solutions of $OSCN^-$ for Figure 2 were prepared by addition of 5 mL TauCl (100 μM) to 5 mL SCN^- (100, 200, and 500 μM) while vortexing over a period of ~1 min. The samples were transferred to 10 mL plastic syringes, the solutions were injected into the 1 m fiber optic cell, and the UV-vis spectra were recorded.

Preparation and Quantification of Ubiquitin Chloramines (Ub*Cl)

Quantitative oxidation of ubiquitin (Ub) Met-1 to a sulfone (Ub*) was accomplished with performic acid using a literature procedure (20). The performic acid was prepared by mixing 0.50 mL of 30 % hydrogen peroxide with 9.5 mL of 99% formic (HCOOH) acid and allowing the mixture to stand for 2 h at room temperature. Before use, this freshly-prepared performic acid (10 ml) was pre-cooled to 0 °C (ca. 1 mL of methanol was added to the reagent to prevent freezing). Ub (3.0 mg) was dissolved in the performic acid (3.0 mL), the mixture was allowed to stand for 4 h at 20 °C, and cold HBr (2.0 ml of 48%) was added to destroy the excess performic acid. The volatiles were removed using a rotary evaporator at 37°C, and the residue was re-dissolved in 0.10 M phosphate buffer at pH 7.4. Oxidized ubiquitin (25 μM Ub*, as determined by the absorption at 280 nm) was treated with OCl^- (250 μM) for various amounts of time (0–2 hours) in 0.1 M phosphate buffer at pH 7.4. The resulting chloramines (Ub*Cl) were quantified with 5-thio-2-nitrobenzoic acid (TNB, λ_{max} = 412 nm, ε_{412nm} = 14,150 $M^{-1}cm^{-1}$). Ub*Cl was incubated with TNB for 3 min before the UV-vis measurements were made. Based on the TNB analysis, 33–41% (n = 3) of the original HOCl oxidizing equivalents were recovered from Ub*Cl.

Reaction of Ub*Cl with SCN^- and Quantification of $OSCN^-$

Equal volumes (5 mL) of 6.8 μM Ub*Cl with 0.50 mM SCN^- were mixed. After 20 min, the Ub*Cl/SCN^- mixture was reacted with TNB (59 μM) in a stopped-flow spectrophotometer with 1:1 mixing in single-mixing mode. The rate constant observed ($3.73 \pm 0.01 \times 10^5$ $M^{-1}s^{-1}$) is consistent with the value that was independently measured for the reaction of TNB with authentic samples of $OSCN^-$. The absorption change (ΔAbs) was constant with the recovery of 80% of the redox equivalents that were measured for Ub*Cl using TNB.

Chlorination of *E. coli* and Quantification of Oxidizing Equivalents

Cultures of *E. coli* (MG1655) were grown from frozen stocks to their terminal density in 15 h at 37 °C in Luria-Bertani medium using a shaking water bath. A portion of the culture (40 ml) was centrifuged (10 min at 5000 *g* and 5 °C), washed twice with 0.1 M phosphate buffer (2 × 4 ml), and the resulting cell pellet was re-suspended in phosphate buffer (4 mL) to give a cell density of ca. 10^9 cells/ml (OD_{600} = 0.76). The cell suspension was treated with OCl^- for a period of time (Table 1). After incubation, the chlorinated cells were centrifuged (10 min at 5000 *g* and 5 °C), the supernatant was removed, and the cells were resuspended in 0.1 M phosphate buffer (4 ml). This washing procedure was repeated three times. Following the final resuspension (10^7 cells/ml), the oxidizing equivalents (i.e., “chlorine cover”) were determined by treating the chlorinated cells with TNB in 0.10 M phosphate buffer for 12 min (Table1).

Reaction of Chlorinated MG1655 with SCN^- and Quantification of $OSCN^-$

Equal volumes (5 ml) of chlorinated *E. coli* (10^7 cells/ml, with an experimentally-determined number of two-electron oxidizing equivalents, *vide supra*) and excess SCN^- were mixed. After 12 min., the cell suspension was filtered through a 0.2 μm polyamide filter. The supernatant was reacted with an excess of TNB in a stopped-flow spectrophotometer with 1:1 mixing in

single-mixing mode. Quantification of $OSCN^-$ was computed from ΔAbs at 412 nm within the timeframe of reaction of $OSCN^-$, as explained in the Results and Discussion, Table 1, and Figure 5.

Results and Discussion

Reaction of Small Molecular Chloramines with Thiocyanate

The mechanisms of nucleophilic reactions of taurine chloramine (TauCl) have been investigated recently by Calvo, *et al.* (21). Thiocyanate was included in that study, but the initial SCN^--derived product of the reaction was not identified (it was speculated to be ClSCN or $(SCN)_2$). In this study, we show that the mechanism is more complicated than previously thought. The second-order rate constant for the reaction of protonated TauCl ($TauClH^+$) with SCN^- was determined by Calvo, *et al.* to be close to the diffusion limit (1.9×10^9 $M^{-1}s^{-1}$) (21). However, the pK_a of $TauClH^+$ is approximately zero (22), so the reaction of TauCl with SCN^- is relatively slow at physiologic pH (128.6 ± 0.1 $M^{-1}s^{-1}$ at pH 7.4). Nonetheless, the rate of reaction of SCN^- with chloramines is comparable to the best biological nucleophiles (e.g., thiolates and thioethers) (21,23).

Based upon our earlier studies of the reactions of electrophilic halogenating agents with SCN^- (8,9), we suspected that the product of the reaction of TauCl with SCN^- was in fact $OSCN^-$. Employing a unique UV-visible spectroscopic signature for $OSCN^-$ (λ_{max} = 376 nm, ε= 26.5 $M^{-1}cm^{-1}$) (10), we found that the reaction of TauCl with SCN^- does indeed produce $OSCN^-$ (Figure 2). Because of the small molar extinction coefficient, in order to employ physiologically relevant concentrations of the reactants, it is necessary to use a spectrophotometric cell with a long (1 meter) pathlength. The data of Figure 2 is for $[TauCl]_0$ = 50 μM and $50 \le [SCN]_0 \le 250$ μM, with chemical yields of $OSCN^-$ of 43–100%. The concentration of oxidant (TauCl) that was used is within the range that might be expected for an immune response (although the oxidant flux, not an absolute concentration, is more relevant *in vivo*). The range of $[SCN^-]$ that was used is comparable to the normal reference values in human physiological fluids (33.5 ± 25.4 and 111.2 ± 92.1 μM in plasma, and 542 ± 406 and 1655 ± 841 μM in saliva, for smokers and non-smokers, respectively) (24). Results similar to those of Figure 2 were also obtained for $[TauCl]_0$ = 80 μM and $0.5 \le [SCN]_0 \le 5$ mM, with chemical yields of $OSCN^-$ of 27–100% (Figure S1).

We have previously observed (10,25) that excess SCN^- is required to cleanly produce $OSCN^-$ using other electrophilic halogenating agents (e.g., HOCl (8) and HOBr (9)), because $OSCN^-$ reacts with the oxidants at competitive rates to produce "over-oxidized" products, *vide infra*. Within the chloramine concentration range we investigated ($[TauCl]_0$ = 50–80 μM), a five- to ten-fold molar excess of SCN^- is required to cleanly produce $OSCN^-$ (Figure 2 and Figure S1). In addition, the amount of excess SCN^- that is required to stoichiometrically produce $OSCN^-$ depends inversely upon the $[chloramine]_0$. For example, when $[SCN^-]$ = 10 mM, the chemical yield of $OSCN^-$ drops from 53 to 13%, when the $[TauCl]_0$ is varied from 250 μM to 2 mM (Figure 3). A similar decrease in yield of $OSCN^-$ is observed if $[TauCl]_0$ is kept constant and the $[SCN^-]$ is decreased (data not shown). These observations indicate that $OSCN^-$ is also capable of reacting with TauCl:

$$RNHCl + OSCN^- + H_2O \xrightarrow{k_2} RNH_3^+ + "O_2SCN^-" + Cl^- \quad (4)$$

The simulation of Figure 3 (see the Supporting Information) yields an estimate of $k_2 \approx 5\times10^3$ $M^{-1}s^{-1}$ for eq 4 at neutral pH, about fifty times larger than the rate constant for SCN^- (eq 3, k_1 = 128.6 ± 0.1 $M^{-1}s^{-1}$ at pH 7.4). To further test this model, we briefly investigated the reaction of TauCl with $OSCN^-$. Unfortunately, using existing methods, $OSCN^-$ is always

prepared in the presence of excess SCN^-, a competing reductant for TauCl. Of the methods available to prepare $OSCN^-$, we have found the LPO-catalyzed oxidation of SCN^- by H_2O_2 to be the most effective means of preparing high concentrations of $OSCN^-$ that are relatively free of excess SCN^- and over-oxidation products (10). The LPO-catalyzed oxidation of 5.0 mM SCN^- by 5.0 mM H_2O_2 produces 3.5 mM $OSCN^-$. Unreacted SCN^- and H_2O_2 remain after catalysis, and the latter can be destroyed by catalase if desired; however, for the present study, because we know that the uncatalyzed reaction of H_2O_2 with SCN^- is very slow (26, 27), and because the effects of catalase on the TauCl (28) and on other components of the reaction (*vide infra*) are unknown, we elected not to add catalase to our stock solution. Figure 4 illustrates the reaction of equimolar concentrations of TauCl and $OSCN^-$ (mixed second-order conditions). The reaction was monitored at two wavelengths, 252 nm (filled circles, λ_{max} for TauCl, ε_{252nm} = 429 $M^{-1}cm^{-1}$) and 376 nm (open circles, λ_{max} for $OSCN^-$, ε_{376nm} = 26.5 $M^{-1}cm^{-1}$). The observed absorption change at 252 nm (ΔAbs(obs) = 0.38 AU) was comparable to the change expected for the consumption of 0.74 mM TauCl (ΔAbs(calc) = 0.32 AU). The observed absorption change at 376 nm (ΔAbs(obs) = 0.008 AU) was about half that expected for the consumption of 0.74 mM $OSCN^-$ (ΔAbs(calc) = 0.019 AU). Since the $[OSCN^-]_0$ was confirmed spectrophotometrically before the reaction was initiated, we attribute the shortfall in absorbance to the concomitant absorption increase of one or more of the products. For the purpose of fitting the data to a mixed second-order rate equation (Figure 4, solid lines), the absorption changes were assumed to be due to the consumption of 0.74 mM of TauCl and $OSCN^-$, respectively. For comparison, the expected kinetic trace for the reaction of 0.74 mM of TauCl with 0.74 mM SCN^- is also illustrated (Figure 4, dashed line). Given the order-of-magnitude difference in absorptivities of TauCl and $OSCN^-$, the data at 252 nm are more precise than the data at 376 nm. Nonetheless, three observations are apparent: 1) the observed reactions are much faster than the rate expected for a reaction of TauCl with SCN^-, 2) the rate that is associated with $-d[OSCN^-]/dt$ (2.8×10^3 $M^{-1}s^{-1}$) is faster than $-d[TauCl]/dt$ (1.2×10^3 $M^{-1}s^{-1}$), and 3) the mixed second-order model incompletely describes the observed kinetics. As evidenced by the second observation, TauCl appears to continue to react after the $OSCN^-$ has been consumed. The computed second-order rate constants are comparable to that estimated from Figure 3 (within factors of 2 and 5, respectively), but for reasons discussed next, we are not confident that the available kinetic data define the rate constant or the mechanism.

The over-oxidized product(s) of $OSCN^-$, depicted as cyanosulfite (O_2SCN^-) in eq 4, remains uncharacterized for the present reaction conditions (although O_2SCN^- has been previously characterized in non-aqueous medium) (29–31). While the relatively simple sequential reaction sequence of eq 3 and eq 4 adequately explains the trends we observe for the kinetics and the chemical yields, we suspect that the rate laws of alternative mechanisms may also explain the available data. Eq 5 describes the stoichiometry of a limiting oxidation of SCN^- by an excess of an electrophilic halogenating agent (e.g., where X^+ is the Cl^+ of HOCl or TauCl):

$$4X^+ + SCN^- + 5\,H_2O \rightarrow 4X^- + SO_4^{2-} + OCN^- + 10\,H^+ \quad (5)$$

X^+ is incapable of further oxidizing SO_4^{2-} or OCN^-. Accordingly, we have at best only described the first two steps of the redox cascade that is defined by eq 5. At least two additional two-electron oxidation reactions, and at least one hydrolysis reaction are necessary to relate the sequence of eqs 3 and 4 to eq 5. The observations of Figure 4 suggest that the formation of transient species that continue to react (e.g., $-d(Abs_{252nm})/dt \neq -d(Abs_{376nm})/dt$, despite the fact that $[TauCl]_0$ and $[OSCN^-]$ were carefully measured independently before the reaction was initiated). One possible explanation for the data of Figure 4 is that the observed absorption changes that are attributed to TauCl (following the consumption of $OSCN^-$) are actually due to a transient species that is produced by the initial oxidation (e.g., O_2SCN^-) that undergoes

subsequent hydrolysis and/or disproportionation reactions. Alternatively, it is possible that one or more of the intermediates of the redox cascade of eq 5 is an efficient scavenger of chloramines and/or $OSCN^-$. For the reaction conditions of Figure 4, such scavenging reactions could produce a non-stoichiometric ratio of the original reactants (leaving behind excess TauCl or $OSCN^-$). For example, SO_3^{2-}, which has previously been observed during the decomposition of $OSCN^-$ (32), and which is known to react efficiently with chloramines, is a possible intermediate in the redox cascade of eq 5, (33–36). Furthermore, we have recently shown that cyanide, another product observed during the decomposition of $OSCN^-$, reacts with $OSCN^-$ to give reactive dicyanosulfide, NCSCN (which is itself an unstable species) (37). Accordingly, a more detailed mechanistic study of the reaction of eq 4 must await a better understanding of the overall redox cascade that is defined by the net reaction of eq 5.

Reaction of Protein Chloramines with Thiocyanate

The low molar absorptivity of the distinguishing UV-vis spectroscopic signature of $OSCN^-$ (Figure 2) precludes using electronic spectroscopy to identify the products of the reactions of protein-derived and cell-derived chloramines with SCN^-. To overcome this challenge, we took advantage of the selectivity of $OSCN^-$ for thiols to develop a "kinetic signature" for the presence of $OSCN^-$. Employing 5-thio-2-nitrobenzoic acid (TNB, λ_{max} = 412 nm, ε= 14,150 $M^{-1}cm^{-1}$) as a colorimetric reagent, and by monitoring the kinetics of its oxidation to the disulfide, we are able to readily identify and quantify the oxidant (Figure 5). This assay was vetted using $OSCN^-$ produced by an enzyme system ($LPO+SCN^-+H_2O_2$) (10), and by using the reaction of TauCl with SCN^-, with independent spectroscopic confirmation of the intermediary $OSCN^-$ (cf. Figure 2, Figure S4, and S5) prior to the subsequent quantification using the TNB kinetic method.

Ubiquitin (Ub), a highly-conserved 8.5 kDa eukaryotic regulatory protein, was selected for our investigation of protein chloramines. The expected order of reaction of Ub residues (# in parentheses) with HOCl is: Met (1) >> Lys (7) > Arg (4) > His (1) > Tyr (1) (38). For our studies, the N-terminal Met of Ub was oxidized up to a sulfone (hereafter Ub*) via a procedure that is known not to affect the structure of Ub (39). While we have obtained similar results for the native Ub (data not shown), employing Ub* circumvents the highly competitive reaction of chloramines with Met-1 (which we have recently shown produces a reactive dehydromethionine derivative) (40). Thus, Ub* was reacted with HOCl at pH 7.4 for various amounts of time, and the number of oxidizing equivalents that were incorporated into the protein (Ub*Cl) were subsequently quantified with TNB. We note that Ub*Cl reacts with TNB with apparent biphasic kinetics (Figure S6). The pseudo-second-order rate constants of ca. 10^3 and 10^4 $M^{-1}s^{-1}$ are comparable to the value of $1.38 \pm 0.08 \times 10^4$ $M^{-1}s^1$ that is observed for the reaction of TauCl with TNB under the same reaction conditions (Figure S3), but these rate constants indicate that chloramines of different reactivities are produced in the protein. If insufficient time is allowed for the reaction of Ub* and HOCl, unreacted HOCl remains (which was quantified by its kinetic signature; cf. Figure 5). Once the HOCl is consumed, further delay results in decomposition of the protein chloramines. Once optimized, between 33–41% of the oxidizing equivalents in Ub*Cl (based upon the amount of HOCl) are recovered by its reactions with TNB. The percent recovery we observe is comparable to that reported by Hawkins and Davies for the reaction of plasma proteins with HOCl (41). It is also similar to the maximum of 45% chloramine Pattison, *et al.* recovered from the reaction of lysozyme with HOCl (16). When Ub*Cl is reacted with excess SCN^- and subsequently reacted with TNB, we observe a rate constant ($3.73\pm0.01\times10^5$ $M^{-1}s^{-1}$) that is comparable to that independently measured for the reaction of TNB with authentic $OSCN^-$ (Figure 5) (42,43). In addition, the ΔAbs is what is expected for 80% yield of $OSCN^-$ from the Ub*Cl (based upon the amount of chloramines present).

Reaction of Cellular Chloramines with Thiocyanate

To investigate whether the reaction of eq 3 is observed in cells, we treated *E.coli* (MG1655) cells suspended in phosphate buffer with HOCl to produce a "chlorine cover" (an ill-defined modification of the cells that leaves them with redox-active functionality) (44). Chlorine cover is believed to be the first step in the bactericidal action of active chlorine biocides (e.g., chlorine, hypochlorite, chloramines, etc.). By analogy to the reaction of HOCl with proteins, the modification of cells with HOCl presumably involves the formation of chloramines. To distinguish between cell-associated functionalization and medium-derived chemical species, we employed the following protocol: reaction of 10^9 cells/ml with HOCl for a period of time (Table 1), pelleting by centrifugation and washing with phosphate buffer, reaction of the cells with excess SCN^- for 12 min (Table 1), and filter sterilization through a 0.2 μm polyamide filter. Using this procedure, but without the addition of SCN^-, we were able to recover 33–42% of the two-electron oxidizing equivalents (based upon the original amount of HOCl) upon reaction of the cells with a TNB assay (Table 1 and Figure S8). The assay presumably involves the direct reaction of TNB with cellular chloramines. When SCN^- was included in the assay, we recovered 71–100% as $OSCN^-$ from the supernatant (based upon the two-electron oxidizing equivalents present, 33–42% of the original amount of HOCl) (Table 1 and Figure S9). The latter assay presumably involves the reaction of SCN^- with cellular chloramines to give $OSCN^-$, which is in turn quantified by the TNB.

Biological Significance of the Reduction of Chloramines by SCN^- and $OSCN^-$

Employing experimental rate constants measured for model compounds and concentration estimates, Pattison, *et al.* have recently employed a mathematical model to predict the targets of HOCl in human blood plasma, and to predict the fates of some of the oxidized reactive intermediates (15). Their model provides a suitable starting point for discussing the possible biological significance of the reactions of chloramines with SCN^- and $OSCN^-$. Proteins, free amino acids, lipids, antioxidants, DNA bases, and other potential targets (including SCN^-) were treated as separate classes of biomolecules in the model. It was predicted that HOCl reacts principally with proteins, free amino acids, antioxidants, and SCN^-, with SCN^- being the major individual target (2–8%, depending upon whether the plasma contained 50 or 175 μM SCN^-), but with proteins as a class consuming most of the HOCl (~94%). The computational model predicted that about 5% of the HOCl would produce chloramines, with >80% of the chloramines associated with plasma proteins, and with the remainder associated with small molecules. The model employed by Pattison, *et al.* was an incomplete one, and in particular it employed experimental rate constants for small molecules, not proteins, despite the fact that proteins were a major target of HOCl. Some effort was made to compensate for the anticipated reactivity differences in proteins (e.g., by arbitrarily decreasing the rate constant for protein Met by a factor of 10 relative to free Met), but no effort was made to distinguish between reactions that involve two small molecules, between reactions that involve a small molecule and a protein, or between reactions that involve two proteins. It is reasonable to expect that transhalogenation (and other two-electron redox processes) between two proteins are kinetically disfavored, relative to the reaction pathways that involve two small molecules and small molecules with proteins.

The redox cascade that begins with HOCl produces both chemically inert derivatives (e.g., chlorotyrosine and methionine sulfoxide) and biological reactive intermediates. Chloramines are a major fraction of the reactive secondary derivatives. The present study suggests SCN^- may be particularly effective at scavenging chloramines in protein. The rate constant for the reaction of SCN^- with chloramines (129 $M^{-1}s^{-1}$ at pH 7.4) is comparable to the rate constants for the best proteinaceous nucleophiles Cys (200–900 $M^{-1}s^{-1}$) and Met (40–300 $M^{-1}s^{-1}$) (45). While intra-protein redox reactions are undoubtedly favorable when the protein-derived reaction partners are in close proximity, it is likely that protein chloramines are reactively

isolated from other protein-derived reaction partners will instead find kinetically competent reactions with small molecules. Since small molecular derivatives of Cys and Met are relatively scarce in plasma (10–20 μM) (15), and they are subject to depletion in the presence of HOCl, we suspect that SCN^- may be the major small molecule reductant for protein chloramines *in vivo*. However, SCN^- is also expected to be a major target of HOCl (15). Without thiol reaction partners, $OSCN^-$ may accumulate under conditions of oxidative stress. Further contributing to an expected surplus of $OSCN^-$ is the fact that SCN^- is a major substrate of the myeloperoxidase system for most physiological fluids (ca. eqimolar amounts of HOCl and $OSCN^-$ are produced for $[Cl^-]$ = 100 mM and $[SCN^-]$ = 100 μM) (46,47). An unexpected finding of the present study is the observation that $OSCN^-$ is more reactive towards chloramines than SCN^-. Thus, one fate of $OSCN^-$ that is produced under conditions of HOCl-induced oxidative stress may be as a reductant of chloramines.

Conclusion

We have previously suggested that when available in sufficient quantities, SCN^- might be effective at scavenging HOX (X = Cl and Br) *in vivo* to produce $OSCN^-$ (8,9). The present study evidences the importance of reactions of SCN^- with secondary oxidants that are produced in HOCl-induced redox cascades. Thus, when direct reaction of HOX with SCN^- is inefficient, Cl^+ can be subsequently scavenged by reaction of the resulting chloramines with SCN^-. One surprising result of the present study is the observation that $OSCN^-$ reacts with chloramines faster than SCN^- does. When the chloramines are protein-derived, their reactions with SCN^- and $OSCN^-$ may repair some of the damage that is inflicted by HOCl. We note that it has been previously shown that the biological function of proteins can be lost following side-chain oxidation by HOCl, and chloramines mediate further oxidation reactions and protein unfolding (48). The health/disease consequences of the additional production of $OSCN^-$ from chloramines are unclear. While HOCl and HOBr are more chemically reactive than HOSCN, there is mounting evidence that the production of excess $OSCN^-$ may also have deleterious human health consequences (17,18).

Supplementary Material

Refer to Web version on PubMed Central for supplementary material.

References Cited

1. Winterbourn CC. Reconciling the Chemistry and Biology of Reactive Oxygen Species. Nat. Chem. Biol 2008;4:278–286. [PubMed: 18421291]
2. Pattison DI, Davies MJ. Reactions of Myeloperoxidase-Derived Oxidants with Biological Substrates: Gaining Chemical Insight into Human Inflammatory Diseases. Curr. Med. Chem 2006;13:3271–3290. [PubMed: 17168851]
3. Mainnemare A, Megarbane B, Soueidan A, Daniel A, Chapple ILC. Hypochlorous Acid and Taurine-N-Monochloramine in Periodontal Diseases. J. Dent. Res 2004;83:823–831. [PubMed: 15505230]
4. Venglarik CJ, Giron-Calle J, Wigley AF, Malle E, Watanabe N, Forman HJ. Hypochlorous Acid Alters Bronchial Epithelial Cell Membrane Properties and Prevention by Extracellular Glutathione. J. Appl. Physiol 2003;95:2444–2452. [PubMed: 14514700]
5. Kruidenier L, Kuiper I, Lamers CBHW, Verspaget HW. Intestinal Oxidative Damage in Inflammatory Bowel Disease: Semi-Quantification, Localization, and Association with Mucosal Antioxidants. J. Pathol 2003;201:28–36. [PubMed: 12950014]
6. Krasowska A, Konat GW. Vulnerability of Brain Tissue to Inflammatory Oxidant, Hypochlorous Acid. Brain Res 2004;997:176–184. [PubMed: 14706870]
7. Davies MJ, Hawkins CL, Pattison DI, Rees MD. Mammalian Heme Peroxidases: From Molecular Mechanisms to Health Implications. Antioxid. Redox Signaling 2008;10:1199–1234.

8. Ashby MT, Carlson AC, Scott MJ. Redox Buffering of Hypochlorous Acid by Thiocyanate in Physiologic Fluids. J. Am. Chem. Soc 2004;126:15976–15977. [PubMed: 15584727]
9. Nagy P, Beal JL, Ashby MT. Thiocyanate Is an Efficient Endogenous Scavenger of the Phagocytic Killing Agent Hypobromous Acid. Chem. Res. Toxicol 2006;19:587–593. [PubMed: 16608171]
10. Nagy P, Alguindigue SS, Ashby MT. Lactoperoxidase-Catalyzed Oxidation of Thiocyanate by Hydrogen Peroxide: A Reinvestigation of Hypothiocyanite by Nuclear Magnetic Resonance and Optical Spectroscopy. Biochemistry 2006;45:12610–12616. [PubMed: 17029415]
11. Nagy P, Ashby MT. Reactive Sulfur Species: Kinetics and Mechanisms of the Oxidation of Cysteine by Hypohalous Acid to Give Cysteine Sulfenic Acid. J. Am. Chem. Soc 2007;129:14082–14091. [PubMed: 17939659]
12. Nagy P, Ashby MT. Kinetics and Mechanism of the Oxidation of the Glutathione Dimer by Hypochlorous Acid and Catalytic Reduction of the Chloroamine Product by Glutathione Reductase. Chem. Res. Toxicol 2007;20:79–87. [PubMed: 17226929]
13. Harwood DT, Nimmo SL, Kettle AJ, Winterbourn CC, Ashby MT. Molecular Structure and Dynamic Properties of a Sulfonamide Derivative of Glutathione That Is Produced under Conditions of Oxidative Stress by Hypochlorous Acid. Chem. Res. Toxicol 2008;21:1011–1016. [PubMed: 18447396]
14. Ashby MT. Inorganic Chemistry of Defensive Peroxidases in the Human Oral Cavity. J. Dent. Res 2008;87:900–914. [PubMed: 18809743]
15. Pattison DI, Hawkins CL, Davies MJ. What Are the Plasma Targets of the Oxidant Hypochlorous Acid? A Kinetic Modeling Approach. Chem. Res. Toxicol 2009;22:807–817. [PubMed: 19326902]
16. Pattison DI, Hawkins CL, Davies MJ. Hypochlorous Acid-Mediated Protein Oxidation: How Important Are Chloramine Transfer Reactions and Protein Tertiary Structure? Biochemistry 2007;46:9853–9864. [PubMed: 17676767]
17. Wang Z, Nicholls SJ, Rodriguez ER, Kummu O, Hoerkkoe S, Barnard J, Reynolds WF, Topol EJ, DiDonato JA, Hazen SL. Protein Carbamylation Links Inflammation, Smoking, Uremia and Atherogenesis. Nat. Med 2007;13:1176–1184. [PubMed: 17828273]
18. Lloyd MM, van Reyk DM, Davies MJ, Hawkins CL. Hypothiocyanous Acid Is a More Potent Inducer of Apoptosis and Protein Thiol Depletion in Murine Macrophage Cells Than Hypochlorous Acid or Hypobromous Acid. Biochem. J 2008;414:271–280. [PubMed: 18459943]
19. Thomas ELG, M B, Jefferson MM. Cytotoxicity of Chloramines. Meth. Enzymol 1986;132:569. [PubMed: 3821526]
20. Simpson, RJ. Proteins and Proteomics: A Laboratory Manual. New York: Cold Spring Harbor; 2003. p. 370
21. Calvo P, Crugeiras J, Rios A, Rios MA. Nucleophilic Substitution Reactions of N-Chloramines: Evidence for a Change in Mechanism with Increasing Nucleophile Reactivity. J. Org. Chem 2007;72:3171–3178. [PubMed: 17397221]
22. Antelo JM, Arce F, Calvo P, Crugeiras J, Rios A. General Acid-Base Catalysis in the Reversible Disproportionation Reaction of N-Chlorotaurine. J. Chem. Soc., Perkin 2000;2:2109–2114.
23. Peskin AV, Winterbourn CC. Kinetics of the Reactions of Hypochlorous Acid and Amino Acid Chloramines with Thiols, Methionine, and Ascorbate. Free Radical Biol. Med 2001;30:572–579. [PubMed: 11182528]
24. Tsuge K, Kataoka M, Seto Y. Cyanide and Thiocyanate Levels in Blood and Saliva of Healthy Adult Volunteers. J. Health Sci 2000;46:343–350.
25. Nagy P, Lemma K, Ashby MT. Kinetics and Mechanism of the Comproportionation of Hypothiocyanous Acid and Thiocyanate to Give Thiocyanogen in Acidic Aqueous Solution. Inorg. Chem 2007;46:285–292. [PubMed: 17198438]
26. Wilson IR, Harris GM. "The Oxidation of Thiocyanate Ion by Hydrogen Peroxide. II. The Acid-Catalyzed Reaction". J. Am. Chem. Soc 1961;83:286–289.
27. Wilson IR, Harris GM. "The Oxidation of Thiocyanate Ion by Hydrogen Peroxide. I. The pH-Independent Reaction". J. Am. Chem. Soc 1960;82:4515–4517.
28. Mashino T, Fridovich I. Nadph Mediates the Inactivation of Bovine Liver Catalase by Monochloroamine. Arch. Biochem. Biophys 1988;265:279–285. [PubMed: 3421706]

29. Kornath A, Blecher O, Ludwig R. Synthesis and Characterization of Tetramethylammonium Cyanosulfite, $(CH_3)_4N^+SO_2CN$. J. Am. Chem. Soc 1999;121:4019–4022.
30. Kornath A, Blecher O. Decomposition of Tetramethylammonium Cyanosulfite and Crystal Structures of $[(CH_3)_4N]^+HSO_4^-{\cdot}SO_2$ and $[(CH_3)_4N^+]_2S_2O_7^{2-}$.$2SO_2$. Z. Anorg. Allg. Chem 2002;628:625–631.
31. Jander G, Gruttner B, Scholz G. Behavior of Some Compounds of Quadrivalent and Sexivalent Sulfur in Anhydrous Hydrocyanic Acid. II. Chem. Ber 1947;80:279–289.
32. Pruitt, KM.; Tenovuo, JO., editors. Immunology Series, Vol. 27: The Lactoperoxidase System: Chemistry and Biological Significance. 1985. Editors
33. Yiin BS, Walker DM, Margerum DW. Nonmetal Redox Kinetics: General-Acid-Assisted Reactions of Chloramine with Sulfite and Hydrogen Sulfite. Inorg. Chem 1987;26:3435–3441.
34. Stanbro WD, Lenkevich MJ. Kinetics and Mechanism of the Reaction of Aqueous Sulfite with N-Chloroalanylalanylalanine. Int. J. Chem. Kinet 1984;16:251–258.
35. MacCrehan WA, Jensen JS, Helz GR. Detection of Sewage Organic Chlorination Products That Are Resistant to Dechlorination with Sulfite. Environ. Sci. Technol 1998;32:3640–3645.
36. Jensen JS, Helz GR. Dechlorination Kinetics at Alkaline Ph of N-Chloropiperidine, a Genotoxin in Chlorinated Municipal Wastewater. Water Res 1998;32:2615–2620.
37. Lemma K, Ashby MT. Reactive Sulfur Species: Kinetics and Mechanism of the Reaction of Hypothiocyanous Acid with Cyanide to Give Dicyanosulfide in Aqueous Solution. Chem. Res. Toxicol 2009;22:1622–1628. [PubMed: 19705807]
38. Pattison DI, Davies MJ. Absolute Rate Constants for the Reaction of Hypochlorous Acid with Protein Side Chains and Peptide Bonds. Chem. Res. Toxicol 2001;14:1453–1464. [PubMed: 11599938]
39. Breslow E, Chauhan Y, Daniel R, Tate S. Role of Methionine-1 in Ubiquitin Conformation and Activity. Biochem. Biophys. Res. Commun 1986;138:437–444. [PubMed: 3017328]
40. Beal JL, Foster SB, Ashby MT. Hypochlorous Acid Reacts with the N-Terminal Methionines of Proteins to Give Dehydromethionine, a Potential Biomarker for Neutrophil-Induced Oxidative Stress. Biochemistry. 2009 ACS Just Accepted.
41. Hawkins CL, Davies MJ. Hypochlorite-Induced Oxidation of Proteins in Plasma: Formation of Chloramines and Nitrogen-Centered Radicals and Their Role in Protein Fragmentation. Biochem. J 1999;340:539–548. [PubMed: 10333500]
42. Skaff O, Pattison DI, Davies MJ. Hypothiocyanous Acid Reactivity with Low-Molecular-Mass and Protein Thiols: Absolute Rate Constants and Assessment of Biological Relevance. Biochem. J 2009;422:111–117. [PubMed: 19492988]
43. Nagy P, Jameson GNL, Winterbourn CC. Kinetics and Mechanisms of the Reaction of Hypothiocyanous Acid with 5-Thio-2-Nitrobenzoic Acid and Reduced Glutathione. Chem. Res. Toxicol. ACS ASAP.
44. Gottardi W, Nagl M. Chlorine Covers on Living Bacteria: The Initial Step in Antimicrobial Action of Active Chlorine Compounds. J. Antimicrob. Chemother 2005;55:475–482. [PubMed: 15761074]
45. Pattison DI, Davies MJ. Reactions of Myeloperoxidase-Derived Oxidants with Biological Substrates: Gaining Chemical Insight into Human Inflammatory Diseases. Curr. Med. Chem 2006;13:3271–3290. [PubMed: 17168851]
46. vanDalen CJ, Whitehouse MW, Winterbourn CC, Kettle AJ. Thiocyanate and Chloride as Competing Substrates for Myeloperoxidase. Biochem. J 1997;327:487–492. [PubMed: 9359420]
47. Furtmuller PG, Burner U, Obinger C. Reaction of Myeloperoxidase Compound I with Chloride, Bromide, Iodide, and Thiocyanate. Biochemistry 1998;37:17923–17930. [PubMed: 9922160]
48. Hawkins CL, Davies MJ. Inactivation of Protease Inhibitors and Lysozyme by Hypochlorous Acid: Role of Side-Chain Oxidation and Protein Unfolding in Loss of Biological Function. Chem. Res. Toxicol 2005;18:1600–1610. [PubMed: 16533025]

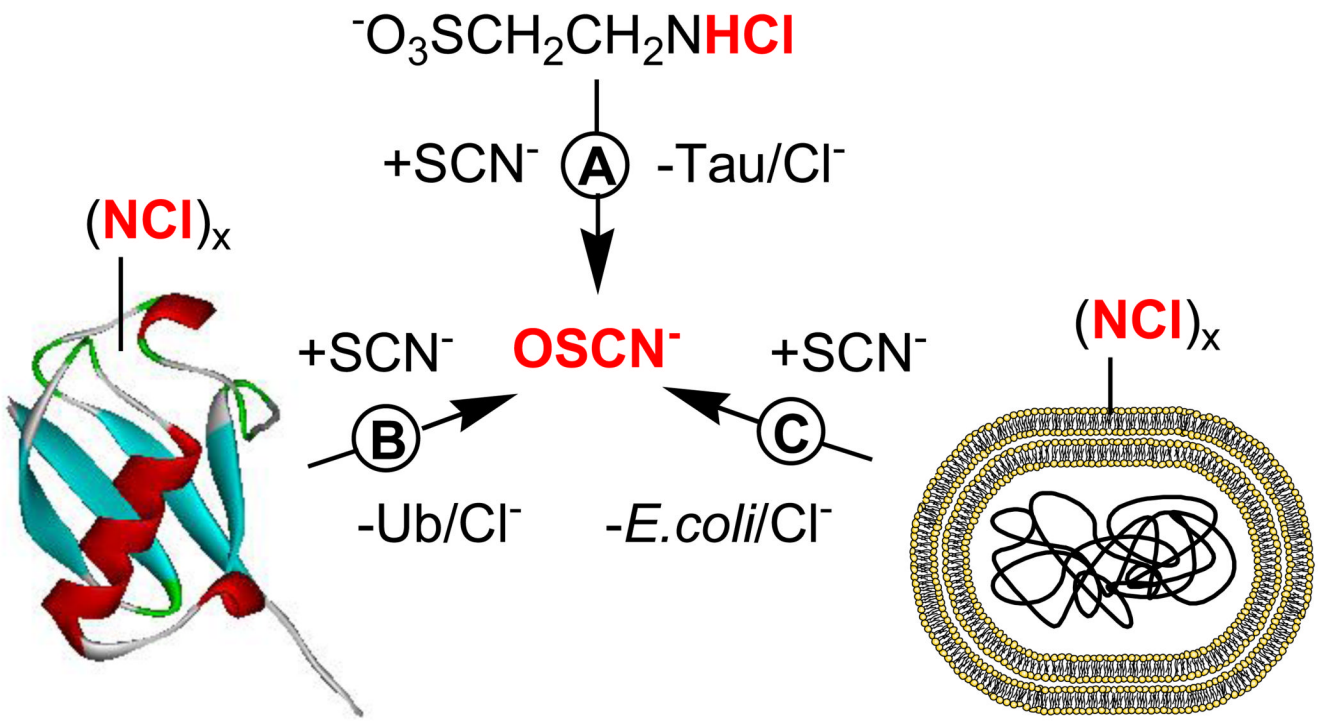

Figure 1.

A) Reaction of taurine chloramine (TauCl) with excess SCN^- gives a quantitative yield of taurine (Tau) and $OSCN^-$. **B)** Reaction of ubiquitin (Ub) with HOCl and subsequent reaction with SCN^- gives $OSCN^-$. **C)** Chlorination of E. coli (MG1655) cells with HOCl, pelleting by centrifugation, suspension in phosphate buffer (to give bacterial cells with "chlorine cover"), reaction of the cells with SCN^-, and filter sterilization through a 0.2 μM polyamide filter yields $OSCN^-$.

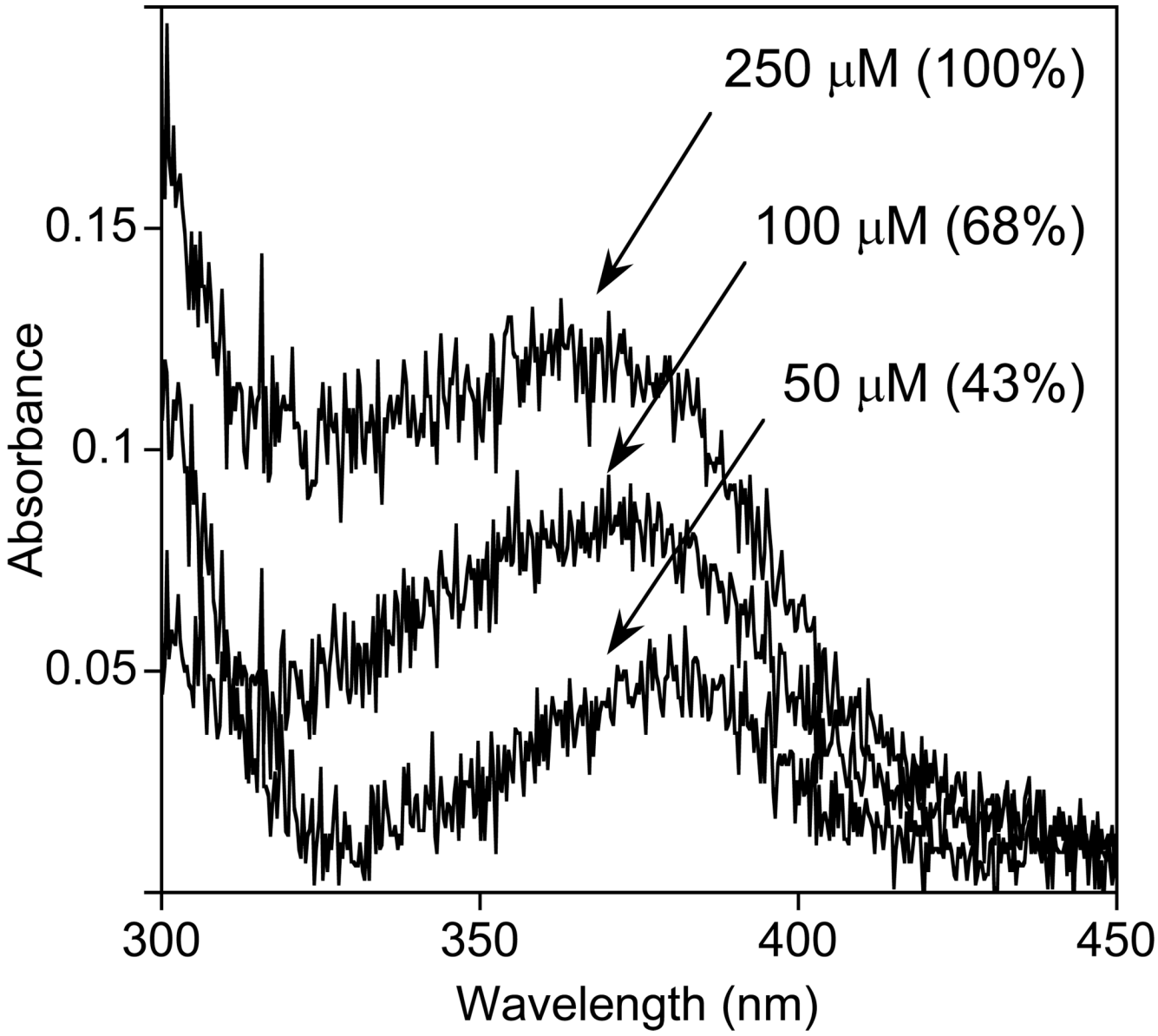

Figure 2.
UV-vis spectra obtained for the reactions of TauCl (50 μM) with SCN^- (50–250 μM) in phosphate buffer (100 mM, pH 7.4) at 20 °C. The spectra were recorded with a 1 meter fiber optic cell. The chemical yield of $OSCN^-$ is indicated versus $[SCN^-]_0$.

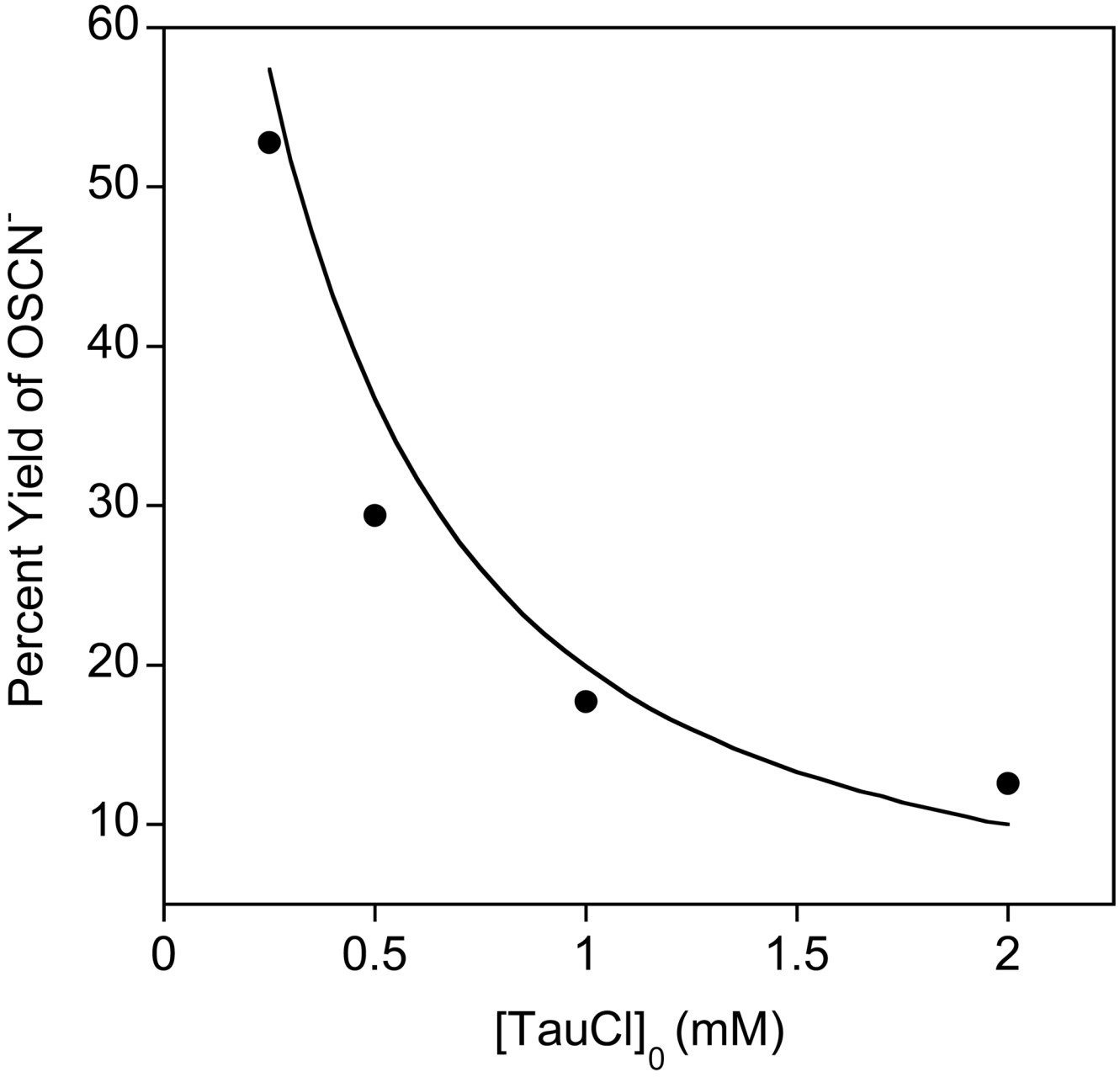

Figure 3.
Chemical yield of $OSCN^-$ for [SCN] = 10 mM and $[TauCl]_0$ = 0.25, 0.50, 1.0, and 2.0 mM in phosphate buffer (100 mM, pH 7.4) at 20 °C.

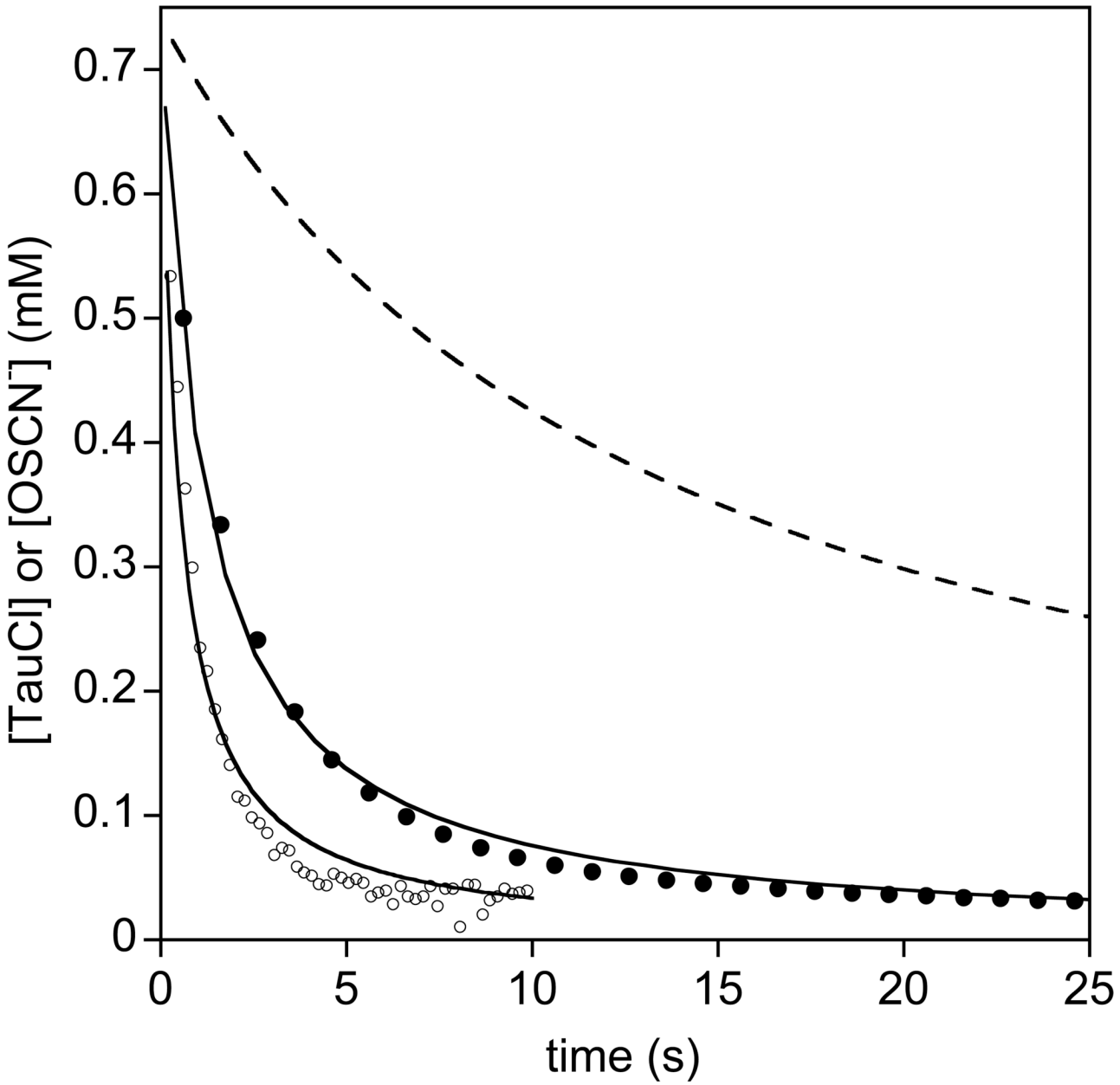

Figure 4.

Concentrations determined at 252 nm (solid circles, λ_{max} for TauCl) and 376 nm (open circles, λ_{max} for $OSCN^-$) versus time for the reaction of $[TauCl]_0$ = 0.74 mM and $[OSCN^-]_0$ = 0.74 mM in phosphate buffer (100 mM, pH 7.4) at 20 °C. The $OSCN^-$ was prepared by the LPO-catalyzed oxidation of 5 mM SCN^- by 5 mM H_2O_2 to give a 3.5 mM stock solution of $OSCN^-$ (determined spectrophotometrically). The solid lines are imperfect non-linear least-squares fit of the experimental data (for clarity, 1% and 10% shown for TauCl and $OSCN^-$, respectively) using a mixed second-order rate equation ($k = 1.182 \pm 0.002 \times 10^3$ and $2.84 \pm 0.03 \times 10^3$ $M^{-1}s^{-1}$ at 276 and 376 nm, respectively). The dashed line is the expected absorption change for a second-order absorption decay for $k = 128.6 \pm 0.1$ $M^{-1}s^{-1}$ (the independently measured rate constant for the reaction of TauCl and SCN^- under the same reaction conditions).

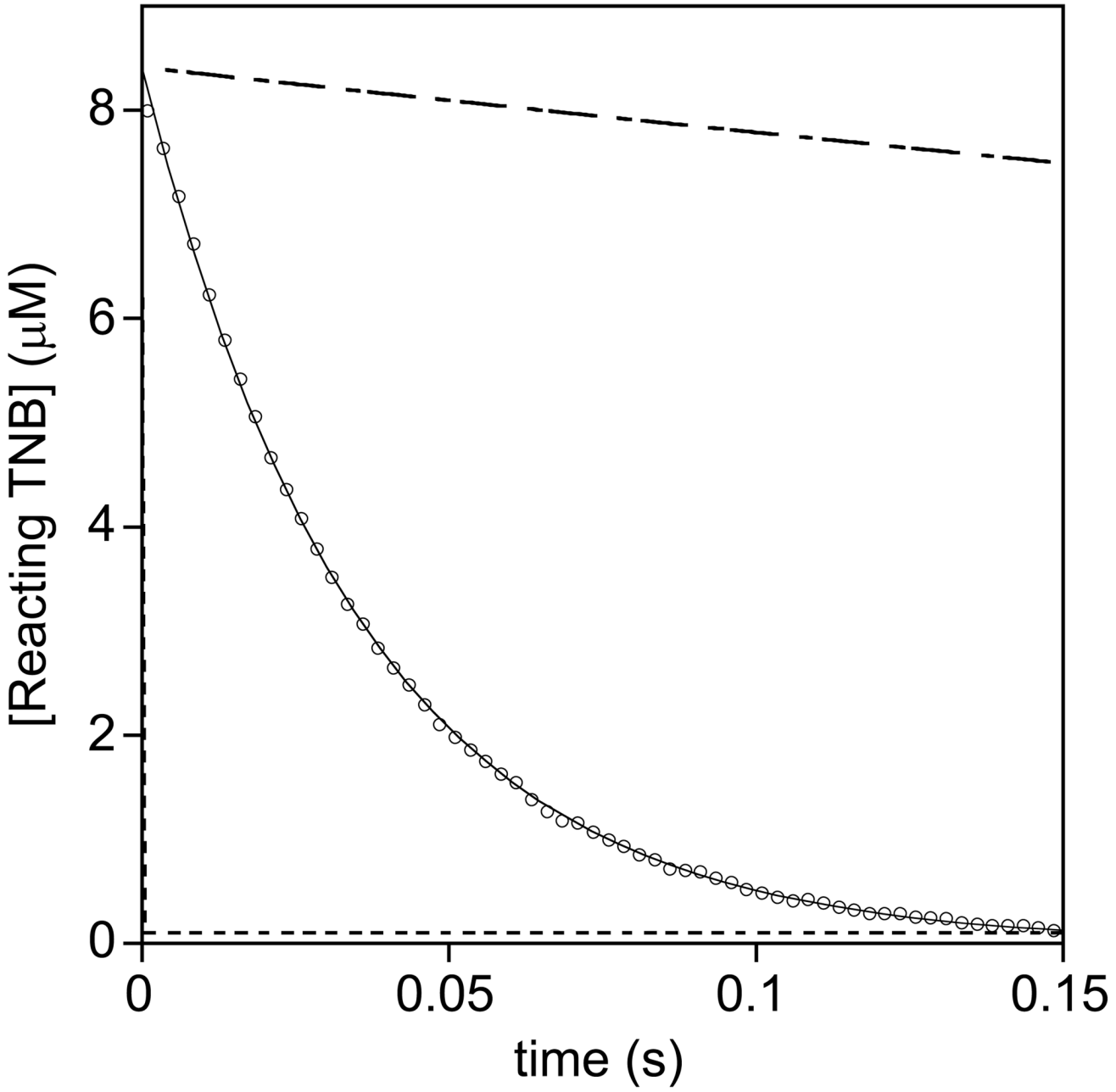

Figure 5.

Kinetic trace for the pseudo-first-order reaction of $OSCN^-$ (4 μM, produced by the LPO-catalyzed oxidation of SCN^- by H_2O_2) with TNB (56 μM) in phosphate buffer at pH 7.4 and I = 1.0 (for clarity, 20 % of the data are illustrated). A non-linear least-squares simulation (shown) yields $k = 5.00 \pm 0.01 \times 10^5\ M^{-1}s^{-1}$. For comparison, simulated traces for the reactions of HOCl (dashed line, $1.9 \pm 0.1 \times 10^9\ M^{-1}s^{-1}$) and TauCl (dot-dashed line, $1.38 \pm 0.08 \times 10^4\ M^{-1}s^{-1}$) with TNB are also illustrated (dashed line). Note that the reaction of HOCl and TNB occurs during stopped-flow mixing, but a subsequent reaction occurs that involves an unidentified intermediate. The rate constants for $OSCN^-$ derived from the reactions of TauCl, Ub*Cl, and chlorinated *E. coli* with SCN^- were $4.44 \pm 0.01 \times 10^5$, $3.73 \pm 0.01 \times 10^5$ and $9.1 \pm 0.1 \times 10^5\ M^{-1}s^{-1}$, respectively.

Table 1

Experimental conditions for reacting *E. coli* cells (10^9 cells/ml) with hypochlorous acid, oxidation equivalents recovered by the TNB analysis, and amount of hypothiocyanite produced upon reaction of the chlorinated cells (10^7 cells/ml) with thiocyanate.

$[HOCl]_0$ (μM)	time of exposure (h)	oxidizing equiv recovered (μM, %)[a]	$OSCN^-$ produced (μM, %)[a]
200	0.5	66 (33)[b]	66 (100)[d,e]
350	0.5	120 (34)[b]	ND
500	0.5	194 (39)[b]	ND
1000	5.0	423 (42)[c]	300 (71)[d,f]

[a] Corrected for a 100-fold dilution of the cells before their reaction with TNB or SCN^-.

[b] $[TNB]_0$ = 74 μM.

[c] $[TNB]_0$ = 61 μM.

[d] Percentage based upon the two-electron oxidizing equivalents recovered by the TNB assay.

[e] $[SCN^-]_0$ = 180 μM.

[f] $[SCN^-]_0$ = 2.5 mM.